ASTFE
American Society
of Thermal and Fluids Engineers

7th Thermal and Fluids Engineering Conference (TFEC)
April - May, 2022
Partially Online Virtual and in Las Vegas, NV Conference

TFEC-2022-41167

CFD PREDICTION OF TURBULENT CONVECTIVE HEAT TRANSFER IN ADDITIVE MANUFACTURED ROUGH CHANNELS

Mohammadreza Kadivar[1,2*], David Tormey[1,2], Gerard McGranaghan[1,2]

[1]Centre for Precision Engineering and Manufacturing Research (PEM Center), Institute of Technology Sligo, Ireland
[2] I-Form, the SFI Advanced Manufacturing Research Center, Ireland

ABSTRACT

Due to the physical phenomena involved in Powder Bed Fusion (PBF) processes, the surface of the manufactured product is naturally rough, significantly impacting the characteristics of fluid flow and heat transfer over the surface. Several studies have attempted to develop Computational Fluid Dynamics (CFD) models to predict friction factor and Nusselt number in rough channels and despite progress in roughness models, further investigations are required to develop a numerically reliable method in the study of heat transfer over the highly irregular roughness made by PBF. This study developed a high-fidelity numerical model based on the Reynolds-Averaged Navier-Stokes (RANS) framework to investigate convective heat transfer over rough surfaces with different roughness heights and topology. Several models based on roughness extensions of RANS were compared with the resolving-roughness approach proposed in this study. In comparison with experimental results, the predictions of this approach broadly match the of the velocity profile for a wide range of roughness heights. The proposed approach predicted the expected downward shift in both the velocity and temperature profiles due to roughness, and the variations of these profiles for different roughness topologies.

KEYWORDS: Convection heat transfer, Computational fluid dynamics (CFD), Turbulent flow, Roughness, Additive Manufacturing, Heat transfer enhancement

1. INTRODUCTION

Additive Manufacturing (AM) is a fast-growing sector that has seen wide adoption in many areas in manufacturing over the past few decades. Of all AM methods, Powder Bed Fusion (PBF) including Direct Metal Laser Sintering (DMLS) are leading technologies in the creation of metallic devices, enabling the fabrication of complex shapes in a single step process [1]. AM has found application in the fabrication of functional cooling channels for gas turbine blades [2], integration of conformal cooling of injection moulding tooling [3], and novel heat exchangers [1]. Due to the nature of the melting process of the metal powder, irregular high roughness is generated on the surface finish [4,5]. This roughness can significantly influence the transport phenomena, such as momentum and heat transfer, of fluids passing over the surface by altering the velocity profile and turbulent properties [6,7]. Despite the extensive published research, convective heat transfer over rough surfaces is not yet fully understood [6]. Several experimental studies have investigated the impact of roughness on friction factor and Nusselt number in channels fabricated by PBF. Ventola et al. [8] reported a maximum of 73% heat transfer enhancement (63% on average) on the AM rough surfaces (fabricated by PBF) compared to smooth surfaces. They reported that the heat transfer enhancement could not be related to the increased roughness area. Stimpson et al. [9,10] reported heat transfer enhancement and pressure drop increase in microchannels fabricated by PBF; however, the Nusselt number increase was not proportional to the rise in the friction factor, especially in channels with small hydraulic diameters [9].

*Corresponding Author: mohammadreza.kadivar@mail.itsligo.ie

Computational Fluid Dynamics (CFD) has been widely used to study turbulent fluid flow and heat transfer. The preponderance of studies being devoted to extending the available turbulent models to account for roughness. These models were developed by applying a negative velocity shift to the classical logarithmic law to fit the mean velocity profile of the rough-wall flow to the experimental data [6,7,11]. Aupoix [12,13] developed a roughness extension to account for high roughness by altering the wall boundary condition of k and ω in SST k-ω models. Recently Mazzei et al. [14,15] calibrated the Aupoix model to calculate friction factor and Nusselt number in AM cooling channels. Roughness models developed based on the logarithmic law can be significantly influenced by the value of equivalent sand-grain roughness height, whose definition and determination are varied [6].

Another approach is the direct resolving of roughness in CFD, known as the roughness-resolving approach. This approach is usually used coupled with scale-resolving methods such as Direct Numerical Simulation (DNS) or Large Eddy Simulation (LES) [16] although suffers from high computational effort [17]. The computational effort can be reduced by coupling the roughness-resolving with Reynolds-Averaged Navier Stokes (RANS) models. Hanson et al. [18] and McClain et al. [19] implemented Spalart-Allmaras and SST k-ω models with the method of Chamenson et al. [20] for generating random analogue roughness using ellipsoid elements. An over-prediction of approximately 50% compared to experimental data for friction factor was reported, resulting from the nature of the ellipsoid analogue surface, which is not suitable for RANS turbulent models.

Since each roughness topography has a distinctive impact on flow, the available methods for predicting drag and heat transfer remain unreliable, with uncertainties costing billions of dollars per year [7]. There is a gap in the literature for a reliable and computationally economical CFD model for rough-wall flow and heat transfer. Therefore, this study evaluated the accuracy of roughness extensions by comparing the CFD results with experimental results of the velocity profile over additive manufactured roughness. A model for roughness-resolving coupled with RANS was proposed to enhance the prediction accuracy of convection heat transfer over rough surfaces, including AM roughness.

2. CFD METHOD

2.1 Reynolds-Averaged Navier Stokes (RANS) The conservation of mass, momentum and energy in RANS framework steady-state Newtonian incompressible flows can be described as [21]

$$\frac{\partial u_j}{\partial x_j} = 0 \tag{1}$$

$$\bar{u}_i \frac{\partial u_j}{\partial x_j} = \frac{\partial}{\partial x_j}\left[\left(\frac{2}{3}k - \frac{p}{\rho}\right)\delta_{ij} + (\frac{\mu + \mu_t}{\rho})\left(\frac{\partial u_i}{\partial x_j} + \frac{\partial u_j}{\partial x_i}\right)\right] \tag{2}$$

$$u_i \frac{\partial T}{\partial x_j} = \frac{\partial}{\partial x_j}\left[\frac{1}{\rho}\left(\frac{\mu}{Pr} + \frac{\mu_t}{Pr_t}\right)\frac{\partial \bar{T}}{\partial x_j}\right] \tag{3}$$

where x_i with i = 1, 2, 3 representing each Cartesian direction. Pr_t is the turbulent Prandtl number considered to be constant at $Pr_t = 0.85$. The turbulent kinetic energy k and the eddy viscosity μ_t were calculated by Shear-Stress Transport (SST) k-ω proposed by Menter [22], a detailed formulation of which can be found in References [22,23].

2.2 Roughness models The most widely used approach for roughness-modelling is based on the equivalent sand grain roughness (ESGR), i.e. a packed layer of spheres of diameter h_s with the same flow characteristics as the actual roughness [6,7]. In CFD and turbulent modelling, especially when using the RANS framework, the effect of roughness is usually modelled by introducing a negative shift of the logarithmic velocity profile, defined as [6,7]

$$U^+ \equiv \frac{U}{U^*} = \frac{1}{\kappa}\ln y^+ + C - \Delta U^+ \tag{4}$$

where $y^+ (= yU^*/\nu)$ is the dimensionless wall distance (y is normal wall distance), C is the smooth-wall intercept (C=5.1), κ is the von Kármán constant ($\kappa \approx 0.41$), and $U^* (= \sqrt{\tau_w/\rho})$ is the friction velocity. The velocity shift ΔU^+, referred to as roughness function, can be calculated by

$$\Delta U^+ = \begin{cases} 0 & h_s^+ \le h_{\text{Smooth}}^+ \\ \frac{1}{\kappa}\ln[C_s h_s^+] \times \sin\left(\frac{\pi}{2}\frac{\ln h_s^+ - \ln h_S^+}{\ln h_R^+ - \ln h_S^+}\right) & h_{\text{Smooth}}^+ < h_s^+ \le h_{\text{Rough}}^+ \\ \frac{1}{\kappa}\ln[C_s h_s^+] & h_s^+ > h_{\text{Rough}}^+ \end{cases} \tag{5}$$

where C_s is the roughness constant and depends on the type of roughness, suggested to be set 0.5, while $h_{\text{Smooth}}^+ = 2.25$ and $h_{\text{Rough}}^+ = 90$.

Aupoix [12] proposed another approach, known as the high roughness model (HRM), that accounts for the effect of roughness by modifying the boundary conditions of k and ω on the surface as

$$k_w^+ = \max\left\{0, \frac{1}{\sqrt{\beta^*}}\tanh\left[\left(\frac{\ln\frac{h_s^+}{30}}{\ln 10} + 1 - \tanh\frac{h_s^+}{125}\right)\tanh\frac{h_s^+}{125}\right]\right\} \tag{6}$$

$$\omega_w^+ = \frac{300}{(h_s^+)^2}\left(\tanh\frac{15}{4h_s^+}\right)^{-1} + \frac{191}{h_s^+}\left[1 - \exp\left(-\frac{h_s^+}{250}\right)\right] \tag{7}$$

where $k_w^+ = k_w/U^{*2}$, $\omega_w^+ = \omega_w\mu/(\rho U^{*2})$, $h_s^+ = \rho\, h_s U^*/\mu$, and $\beta^* = 0.09$. The HRM has been employed in several rough-wall flow studies and was assessed by Mazzei et al. [14,15] for AM rough channels where it show that HRM was an important development from the ESGR method in the prediction of friction factor and Nusselt number. In the present paper, the performance of the HRM and ESGR method in the calculation of velocity profile of flow over roughness were compared. Several correlations have been proposed to evaluate h_s [6,7] and some of them are listed in Table 1

Table 1. Correlations for estimating the equivalent sand-grain roughness h_s

Authors	Correlation
Flack et al. [24,25]	$h_s = \begin{cases} 4.43R_q(1+R_{sk})^{1.37} & R_{sk} > 0 \\ 2.91R_q(2+R_{sk})^{-0.284} & R_{sk} \le 0 \end{cases}$
Stimpson et al. [26]	$\frac{h_s}{D_h} = 18\left(\frac{R_a}{D_h}\right) - 0.05 \quad \frac{R_a}{D_h} > 0.028$
Mazzei et al. [15]	$\frac{h_s}{D_h} = 26.414\frac{R_a}{D_h} - 0.0856 \quad \frac{R_a}{D_h} > 0.0033$

R_a, R_q, and R_{sk} are roughness statistical parameters. In this study, it is these two models, the ESGR and HRM that will be investigated in predicting the velocity profile in flow over AM generated roughness.

2.3 Roughness generation Surface roughness can be characterized by several statistical moments of roughness profile, including arithmetic-averaged height R_a, the root-mean-square roughness (R_q), skewness (R_{sk}) and finally, kurtosis (R_{ku}) [6]. The main constraint of the roughness resolving approach is developing a model to generate roughness topology [18] based on the specified roughness statistics. In this study, the method proposed by Patir [27], and the fast Fourier transform technique were used to generate a matrix of heights with a Gaussian

profile. A Gaussian profile with a given roughness height has $R_{sk} = 0$ and $R_{ku} = 3$. Subsequently, a filtering method based on Johnson's transform system [28] was implemented to convert the Gaussian height matrix to a random matrix of heights with specified roughness parameters. This generated height matrix, also known as a heightmap, can then be used to create a mesh surface, representing the rough surface. Table 2 demonstrates the model's capability in generating rough surfaces using given roughness parameters. The accuracy of the method was evaluated by employing Normalised Root Mean Square Error (NRMSE) and shown in Table 2. The method has the capacity to generate surfaces with an NRMSE of 0.49, 5.65, and 5.63 to achieve the specified R_q, R_{sk}, and R_{ku}, respectively. The accuracy can be further enhanced by using a larger matrix of heights for roughness but will increase the computational effort in CFD.

Table 2. Correlations for estimating the equivalent sand-grain roughness h_s

Surface	Input parameters				Parameters of generated surface			
	R_a (μm)	R_q (μm)	R_{sk}	R_{ku}	R_a (μm)	R_q (μm)	R_{sk}	R_{ku}
Gaussian	11.00	13.00	0.00	3.00	10.35	13.08	-0.03	3.24
Negatively Skewed	11.00	13.22	-1.00	3.00	10.92	13.22	-1.01	2.97
Platykurtic	11.00	13.00	0.00	1.50	11.61	12.92	0.01	1.52
NRMSE (%)					4.72	0.49	5.65	5.63

2.4 Numerical procedure and validation The Finite Volume Method (FVM) with pressure-velocity coupled algorithm was employed in ANSYS fluent 19.2 to solve the governing equations. The second-order upwind method was applied to discretise the transport equations. The convergence of the numerical solution was assured by monitoring the normalized residuals to reach a constant level below 10^{-6} for each variable.

$$y^+ = U^+ + \exp(-\kappa c)\left[\exp(\kappa U^+) - 1 - \sum_{n=1}^{4}\frac{(\kappa U^+)^n}{n!}\right] \tag{8}$$

$$Nu = \frac{(f/8)(Re - 1000)Pr}{1 + 12.7(f/8)^{1/2}(Pr^{2/3} - 1)}, \quad f = (0.79\ln Re - 1.64)^{-2} \tag{9}$$

The numerical code was validated by comparing the CFD results with experimental data for the fully developed convection heat transfer in a smooth channel. Fig. 1 (a) shows that the CFD predictions agree with Spalding law [29], Eq. (8) with an close agreement of velocity profile in the viscosity affected region. Fig. 1 (b) shows good agreement the CFD code for with the Gnielinski [30] correlation for Nusselt number in smooth channels, , Eq (9).

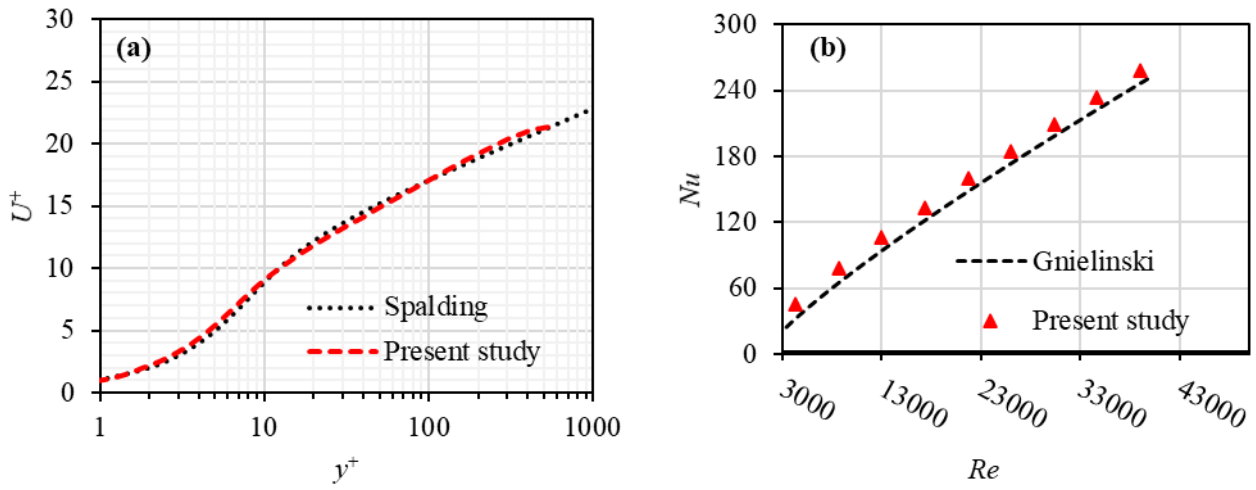

Fig. 1 Validation with (a) velocity profile of Spalding [29]; and (b) Nusselt number of Gnielinski [30].

3. RESULTS AND DISCUSSION

3.1 Evaluation of roughness models The roughness models eliminate the need to include the geometry of roughness in CFD by using added models accounting for roughness. The experimental velocity profile from the study of McClain et al. [19] was used to evaluate the models. They recorded the fully developed velocity profile in a rough channel with AM roughness fabricated by PBF technology.

Fig. 2 (a) shows the schematic of the air-flow experiment of McClain et al. [19]. The actual dimensions of the channel cross-section dimensions of W = 228.6 mm, H = 35.56 mm, but a different length of 200 mm (using periodic boundary for inlet and outlet) were employed in the CFD. The bottom surface of the channel was the rough test surface, while the other top and lateral walls were smooth. The difference between geometries used in roughness-modelling approaches (ESGR and HRM) and the roughness-resolving approach is schematically illustrated in Fig. 2 (b), along with the mesh strategies. A Periodic boundary condition was applied to the inlet and outlet of the channel to ensure fully developed flow in the channel, and the no-slip boundary condition was used on the smooth surfaces of the channel. The boundary condition on the rough surface was specified based on the roughness model, as described in section 2.2. The computational grids consisted of polyhedral elements with sizing of 100 × 100 × 100 cells, and the first node was positioned at a distance of 1×10^{-6} m from the wall to ensure $y^+ < 1$. A mesh dependency analysis was performed with sizing of 150 × 150 × 150 cells and showed no noticeable change in the velocity profile, as illustrated in Fig 2 (c).

McClain et al. [19] investigated three different rough surfaces, named Real_x102, Downskin, and Upskin, with specifications listed in Table 3. The value of h_s was calculated using different correlations (see Table 1) listed in Table 3, with h_{s_F}, h_{s_S}, and h_{s_M} representing the value of equivalent sand-grain roughness height corresponding to the respective correlations of Flack et al. [24,25], Stimpson et al. [26], and Mazzei et al. [15],. Fig. 3 compares the CFD results with the experimental velocity profile of McClain et al. [19] for the channel with Real_x102 rough surface. Since the overall pressure gradient in the streamwise direction is balanced, the bulk flow is shifted towards the wall having the lower frictional resistance (smooth wall); therefore, Fig. 4 demonstrates a velocity shift towards the smooth surface. Both ESGR and HRM provided good predictions of the velocity shift toward the smooth wall and also the position of the maximum velocity.

For the Real_x102 surface (with the highest roughness), the HRM model displays better agreement than the ESGR model in the velocity profiles. Using the h_{s_M}, h_{s_S}, and h_{s_F} values, the HRM presented NRMSEs of 14.7 %, 15.6 %, and 24.5 %, respectively, and the corresponding NRMSEs of the ESGR model were 26.9 %, 36.8 %, and 39.5 %, respectively. For the Downskin surface, the HRM provided slightly better predictions than the ESGR model with an NRMSE of about 19.0 % for HRM and about 21.5 % for ESGR.

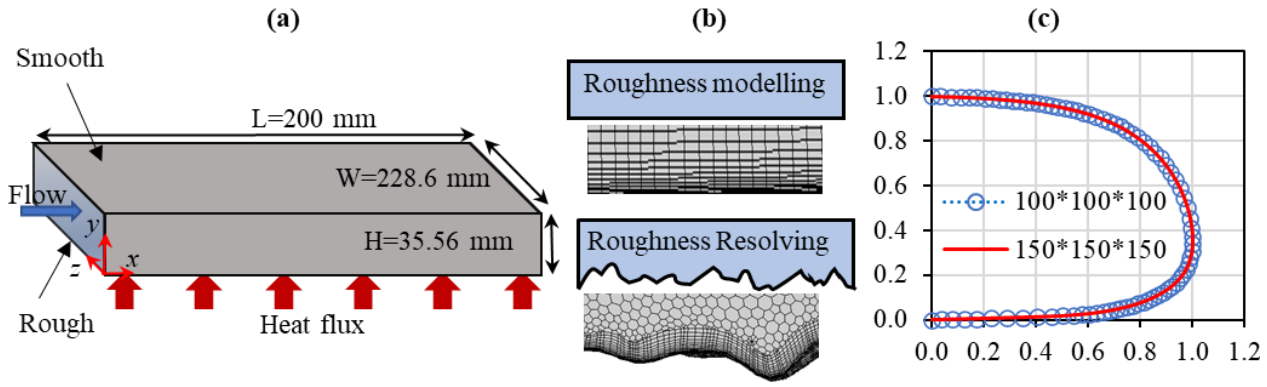

Fig. 2 (a) Geometry used in CFD based on McClain et al. [19] experiment (b) schematic of the cross-section of channels in roughness-modelling and roughness-resolving approaches and the mesh near the surface for roughness modelling (top) and roughness-resolving (bottom) (c) mesh dependency analysis (Upskin surface).

Table 3 Rough surfaces used in McClain et al. [19] study.

Surface	R_a (mm)	R_q (mm)	R_{sk}	h_{s_F} (mm)	h_{s_S} (mm)	h_{s_M} (mm)
Real_x102	1.887	2.436	-0.276	6.07	30.89	44.57
Upskin	0.303	0.386	0.195	2.12	2.38	2.74
Downskin	0.737	0.936	0.082	4.48	3.64	4.58

The HRM and ESGR models performed almost equally in predicting velocity profile over the Upskin surface (with the lowest roughness), representing an NRMSE of roughly 9.7 % for HRM and about 7.0 % for ESGR. This demonstrates that the ESGR model is better suited for surfaces with low roughness, while for surfaces with high roughness, the HRM appears to provide predictions closer to experimental measurements. These findings agree with the results of Mazzei et al. [14,15] where the HRM was an important step ahead of the ESGR model.

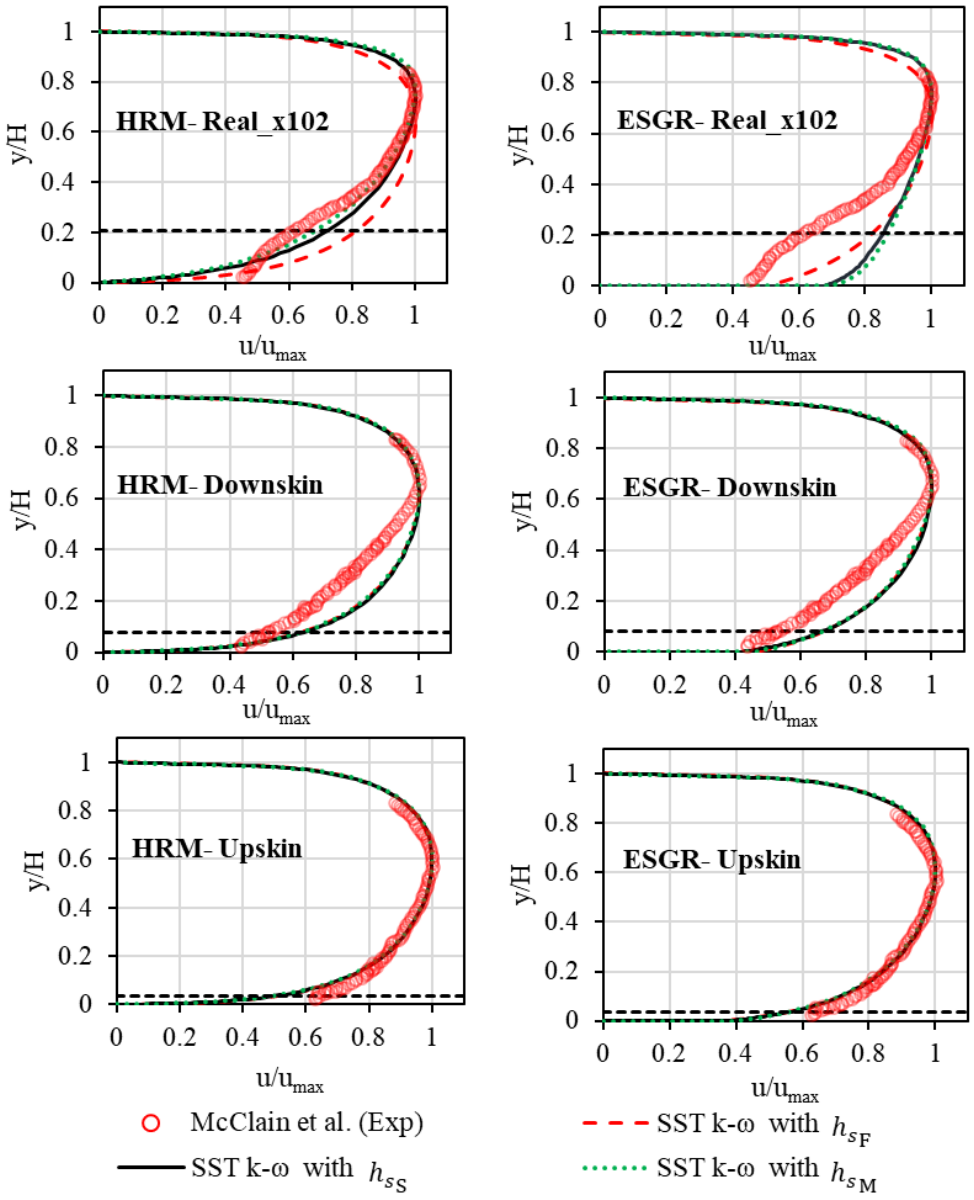

Fig. 3 Comparison of CFD results of roughness models (ESGR and HRM) with the experimental velocity profile of McClain et al. [19]. The horizontal dashed lines show the maximum extent of roughness.

The main limitation of roughness models is their dependence on the variance associated with the determination of h_s. As shown in Fig.3, the predictions of the model are significantly influenced by the method of determining h_s. For the Real_x102 surface, all three h_s values are seen to perform close to the general form of the experimental data at y/H values of around 0.6 - 0.8. However, all three are seen to deviate from the experimental results at values above or lower. The Stimpson et al. correlation provided better predictions of the h_s value likely as it was based on experimental friction factor data from rough microchannels fabricated by PBF. The Mazzei et al. correlation is a revised version of the Stimpson et al. correlation, intended to improve the original by better fitting the experimental data with the HRM and it can be seen to agree more closely with the experimental results in HRM. The Flack et al. correlation was predominantly formulated from studies on surfaces with sparse roughness elements; therefore, underpredicts the h_s value, leading to the underestimation of the roughness effect on the velocity profile. It appears to be less suited for AM surfaces with high density roughness All three h_s values exhibit some difference from experimental results, especially in the region near to the rough wall.

As illustrated in Fig. 3, all correlations provide similar results for Upskin and Downskin surfaces due to the closeness in values calculated for h_s. However, by increasing the roughness height, each correlation yields different values of h_s. Therefore, for the Real_x102 surface, the predicted velocity profile varies with the type of correlation used for h_s. Compared to the experimental results, the Flack et al. correlation underpredicts the h_s values of AM roughness, leading to underprediction of the velocity shift and the position of the maximum profile for flow above the Real_x102 surface. HRM provided closer predictions to the experimental results by using Stimpson et al. and Mazzei et al. correlations, although the better result was found by employing the Mazzei et al. correlation.

3.2 Evaluation of resolving-roughness approach The CFD simulations explained in the previous section were replicated using resolving-roughness with RANS (SST k-ω) and employing the actual geometry of roughness generated by the method explained in section 2.3. An unstructured polyhedral mesh with 30 boundary layer mesh was used and the first layer was positioned at a distance of 1×10^{-6} m from the wall to ensure a $y^+ < 1$. A mesh dependency analysis was performed by increasing the number of computational cells and comparing the resulting velocity profile until no noticeable changes were observed. A computational grid with 7,120,900 cells for channels with Upskin surface, 7,630,249 cells for Downskin surface, and 11,854,532 cells for Real_x102 surface were found to be sufficient for this study.

Fig. 4 illustrates the CFD results of resolving-roughness with RANS (SST k-ω) compared with the experimental velocity profiles of McClain et al. [19]. A noticeable improvement in the prediction of the velocity profile for all surfaces is observed compared to the roughness-modelling approach.

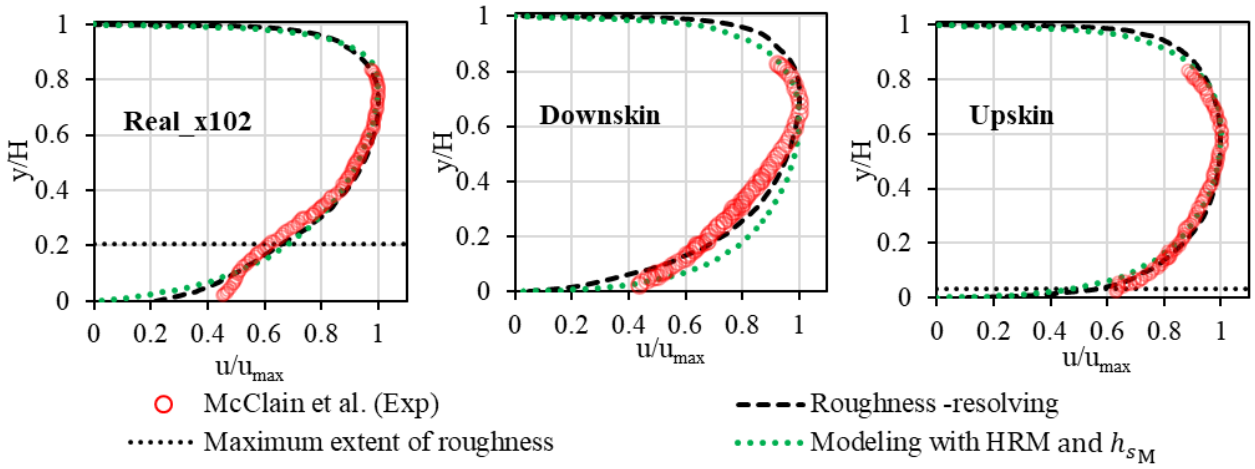

Fig. 4 The CFD results of resolving-roughness with RANS (SST k-ω) compared with the experimental velocity profile of McClain et al. [19].

For Real_x102, Downskin, and Upskin surfaces, the NRMSEs of the resolving-roughness were 7.4 %, 18.5 % and 8.6 %, respectively, and the corresponding NRMSEs of HRM (using Mazzei et al. correlation) were 14.7 %, 19.0 % and 9.7 %, respectively. The velocity profile obtained by resolving-roughness follows the changes in the trends of the experimental velocity and correctly predicts the velocity shift. Although there is slight underprediction in the velocity shift for Upskin and Downskin surfaces, for Real_x102, the model provided a very good prediction of the velocity shift. For Real_x102, both approaches are seen to perform close to the general form of the experimental data at y/H values of larger than 0.3, slight underprediction at y/H values of around 0.1 - 0.3, and large deviation at y/H < 0.1. For Downskin, the roughness resolving approach is found to perform close to the general form of the experimental data at y/H values of around 0.1 - 0.6, while HRM showed better predictions at y/H values of around 0.6 - 0.8. For Upnskin, a close prediction to the general form of the experimental data is found for the roughness-resolving approach at about y/H < 0.6 and for HRM at about y/H > 0.6. Fig 4 demonstrates the capacity of the roughness-resolving approach coupled with RANS for modelling a wide range of roughness heights. The discrepancies of resolving-roughness observed in Fig. 4 could be due to the deficiency of RANS models in the prediction of detached flow, consequently leading to incorrectly maintaining attached flow over the isolated roughness elements. CFD of rough-wall flows is challenging due to three phenomena that exist in such flows: (i) strong favourable pressure gradient on the windward faces of most roughness elements (ii) strong adverse pressure gradient on the leeward faces (iii) expected highly anisotropic turbulence near and between the roughness elements [19]. The evaluation of the roughness models for convective heat transfer, including RHM and ESGR, was recently investigated by Mazzei et al. [14,15]. They reported that HRM is an important step ahead of ESGR for predicting friction factors, but the heat transfer prediction demands the implementation of the thermal correction models. They improve the predictions of RHM by calibrating the thermal correction model of Aupoix [13] using the experimental data of Stimpson et al. [26] for heat transfer in mini-channels fabricated by PBF.

3.3 The effect of roughness parameters on velocity and temperature profiles The roughness-resolving approach eliminates the need to implement thermal corrections for prediction of heat transfer in CFD. This approach also includes the effect of increased heat transfer area from the roughness. In order to reduce the computation effort, further CFD simulations were performed in a smaller channel (a mini-channels) with the configuration shown in Fig. 2, a cross-section of 2 mm × 1 mm, and a length of 3 mm. A heat flux of 20 W/cm^2 was applied to the bottom surface of the channel. In order to evaluate the influence of the roughness topology on the temperature and velocity profile, the Gaussian, Negatively Skewed, and Platykurtic surfaces (with similar R_q but different R_{Sk} and R_{ku}) listed in Table 2 were simulated using the roughness-resolving approach. Fig. 5 illustrates the expected shift in velocity and temperature profiles at Re = 15000 for these different surfaces. The velocity shift of the Negatively Skewed rough surface is lower than that of other rough surfaces showing smaller friction drag over Negatively Skewed surface due to removed roughness peaks. However, the velocity profile of the Platykurtic surface behaves similarly to the Gaussian surface for $y^+ > 100$, showing that the effect of kurtosis on the friction drag is marginal. Fig 5 (b) demonstrates the capability of the roughness-resolving approach in predicting negative temperature shifts due to roughness. The Smooth, and Gaussian and Negatively Skewed have similarly positioned trends to the velocity profiles, apart from Platykurtic, which is demonstrably lower.

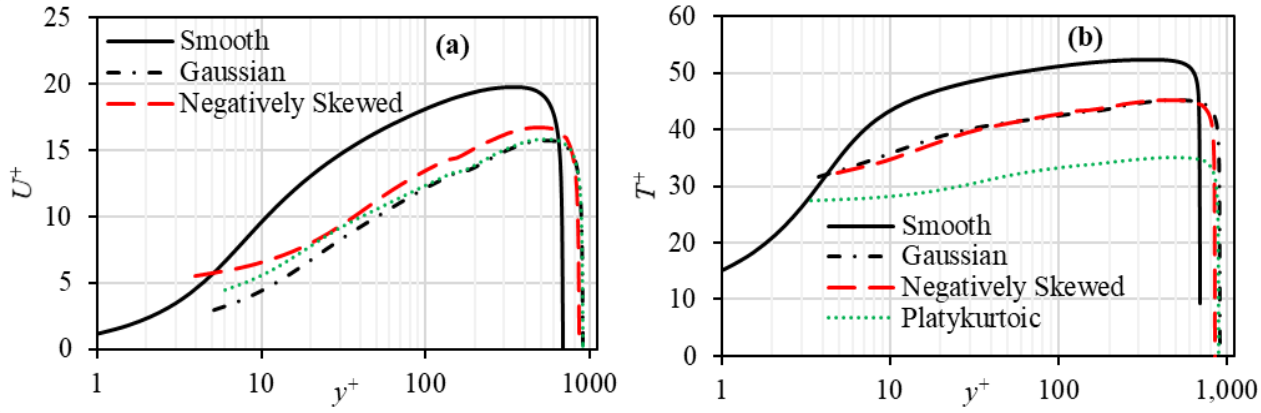

Fig. 5 (a) velocity profile and (b) temperature profile for Gaussian, Skewed, and Platykurtic surface at Re=15000.

4. CONCLUSIONS

This study evaluates the predictions of the roughness-resolving approach and common roughness-modelling methods in the RANS framework in predicting flow and heat transfer over additive manufactured rough surfaces. The CFD results were compared with experimental data of velocity profiles over rough surfaces fabricated by PBF technology.

For roughness-modelling methods, HRM is an important step ahead of ESGR in predicting the velocity profile. From the observations in this study, the ESGR model appears to best suit surfaces with low roughness, while HRM can provide more accurate predictions for surfaces with high roughness. The main drawback of roughness models relies on the uncertainty associated with the values of equivalent sand-grain roughness heigh, h_s. The performance of several correlations (proposed by Flack et al. [24,25], Stimpson et al. [26], and Mazzei et al. [15]) in the prediction of h_s values for AM roughness were compared. The predicted value of h_s by all correlations led to similar predictions of the velocity profile for low roughness; however, for higher roughness, the values of Mazzei et al. correlation were closer to the experimental data. The prediction of heat transfer by roughness models requires the adoption of a calibrated thermal correction model [15]. Further analyses considering different geometry, roughness, fluid, and flow conditions would be required to improve the roughness models.

A method for actual roughness generation was proposed, and the performance of the roughness-resolving approach coupled with SST k-ω was evaluated. This approach demonstrated better performance in predicting the experimental velocity profile than that of the roughness models (HRM and ESGR). The predictions of this approach broadly matched the experimental results of the velocity profile for a wide range of roughness height studies. The combination of roughness-resolving with RANS predicted the negative temperature shift due to roughness without the inclusion of thermal correction models. The results demonstrated that, apart from roughness height, the skewness and kurtosis of roughness also influence the velocity and temperature profile. The roughness-resolving with RANS approach has the capacity to predict heat transfer and fluid dynamics in rough channels fabricated by additive manufacturing, albeit requiring more computational effort than roughness models. For more complex rough channels, such as conformal cooling channels, the HRM coupled with a thermal correction model can be used although the proper correlation must be used to estimate the h_s value.

ACKNOWLEDGMENT

This research is supported by an IT Sligo Bursary and also by a research grant from Science Foundation Ireland (SFI) under Grant Number 16/RC/3872 and is co-funded under the European Regional Development Fund and by I-Form industry partners. The authors wish to acknowledge the Irish Centre for High-End Computing (ICHEC) for the provision of computational facilities and support.

NOMENCLATURE

h_s	Equivalent sand-grain roughness	(mm)	u	Reynolds-averaged velocity	(m/s)
H	Channel's height	(mm)	U	Average velocity profile	(m/s)
k	Turbulent kinetic energy	(m^2/s^2)	U^+	Dimensionless velocity profile	(-)
p	Pressure	(Pa)	U^*	Friction velocity	(m/s)
Pr	Prandtl number	(-)	ΔU^+	Roughness function	(-)
Pr_t	Turbulent Prandtl number	(-)	y^+	Dimensionless distance from wall	(-)
Re	Reynolds number	(-)	τ_w	Wall shear stress	(Pa)
R_a	Arithmetic-averaged height	(μm)	ρ	Density	(kg/m^3)
R_q	Root-mean-square height	(μm)	μ	molecular viscosity	(kg/ms)
R_{sk}	Skewness of roughness	(-)	μ_t	eddy viscosity	(kg/ms)
R_{ku}	Kurtosis of roughness	(-)	ω	Turbulent dissipation rate	(1/s)
T	Reynolds-averaged temperature	(K)			

REFERENCES

[1] Jafari, D., and Wits, W. W., "The Utilization of Selective Laser Melting Technology on Heat Transfer Devices for Thermal Energy Conversion Applications: A Review," *Renew. Sustain. Energy Rev.*, 91, pp. 420–442 (2018).

[2] Kirsch, K. L., and Thole, K. A., "Heat Transfer and Pressure Loss Measurements in Additively Manufactured Wavy Microchannels," *J. Turbomach.*, 139(1), p. 011007, (2017).

[3] Feng, S., Kamat, A. M., and Pei, Y., "Design and Fabrication of Conformal Cooling Channels in Molds: Review and Progress Updates," *Int. J. Heat Mass Transf.*, 171, p. 121082, (2021).

[4] Snyder, J. C., and Thole, K. A., "Understanding Laser Powder Bed Fusion Surface Roughness," *J. Manuf. Sci. Eng.*, 142(7), p. 071003, (2020)

[5] Snyder, J. C., and Thole, K. A., "Tailoring Surface Roughness Using Additive Manufacturing to Improve Internal Cooling," *J. Turbomach.*, 142(7), p. 071004, (2020)

[6] Kadivar, M., Tormey, D., and McGranaghan, G., "A Review on Turbulent Flow over Rough Surfaces: Fundamentals and Theories," *Int. J. Thermofluids*, 10, p 100077, (2021).

[7] Chung, D., Hutchins, N., Schultz, M. P., and Flack, K. A., "Predicting the Drag of Rough Surfaces," *Annu. Rev. Fluid Mech.*, 53(1), pp. 439–471, (2021).

[8] Ventola, L., Robotti, F., Dialameh, M., Calignano, F., Manfredi, D., Chiavazzo, E., and Asinari, P., "Rough Surfaces with Enhanced Heat Transfer for Electronics Cooling by Direct Metal Laser Sintering," *Int. J. Heat Mass Transf.*, 75, pp. 58–74, (2014).

[9] Stimpson, C. K., Snyder, J. C., Thole, K. A., and Mongillo, D., "Roughness Effects on Flow and Heat Transfer for Additively Manufactured Channels," *J. Turbomach.*, 138(5), p. 051008, (2016).

[10] Stimpson, C. K., Snyder, J. C., Thole, K. A., and Mongillo, D., "Effectiveness Measurements of Additively Manufactured Film Cooling Holes," *J. Turbomach.*, 140(1), p. 011009, (2018)

[11] Jiménez, J., "Turbulent Flows over Rough Walls," *Annu. Rev. Fluid Mech.*, 36(1), pp. 173–196, (2004).

[12] Aupoix, B., "Roughness Corrections for the K-ω Shear Stress Transport Model: Status and Proposals," *J. Fluids Eng. Trans. ASME*, 137(2), p. 021202, (2015).

[13] Aupoix, B., "Improved Heat Transfer Predictions on Rough Surfaces" *Int. J. Heat Fluid Flow*, 56, pp. 160–171, (2015).

[14] Mazzei, L., Da Soghe, R., and Bianchini, C., "Calibration of a CFD Methodology for the Simulation of Roughness Effects on Friction and Heat Transfer in Additive Manufactured Components," *Proc. ASME Turbo Expo 2021: Turbomachinery Technical Conference and Exposition*, 5B(V05BT13A010), (2021).

[15] Mazzei, L., Da Soghe, R., and Bianchini, C., "CFD Modelling Strategies for the Simulation of Roughness Effects on Friction and Heat Transfer in Additive Manufactured Component," *Proc. ASME Turbo Expo 2020: Turbomachinery Technical Conference and Exposition*,7C(V07CT13A021), (2020).

[16] Piomelli, U., "Recent Advances in the Numerical Simulation of Rough-Wall Boundary Layers," *Phys. Chem. Earth*, 113, pp. 63–72, (2019).

[17] Thakkar, M., Busse, A., and Sandham, N., "Surface Correlations of Hydrodynamic Drag for Transitionally Rough Engineering Surfaces," *J. Turbul.*, 18(2), pp. 138–169, (2017).

[18] Hanson, D. R., McClain, S. T., Snyder, J. C., Kunz, R. F., and Thole, K. A., "Flow in a Scaled Turbine Coolant Channel with Roughness Due to Additive Manufacturing," *Proc. of the ASME Turbo Expo 2019: Turbomachinery Technical Conference and Exposition*, (2019).

[19] McClain, S. T., Snyder, J. C., Hanson, D. R., Kunz, R. F., Cinnamon, E., and Thole, K. A., "Flow in a Simulated Turbine Blade Cooling Channel with Spatially Varying Roughness Caused by Additive Manufacturing Orientation," *J. Turbomach.*, 143(7), p. 071013 (2021).

[20] Clemenson, J. M., Shannon, T. A., and McClain, S. T., "A Novel Method for Constructing Analog Roughness Patterns to Replicate Ice Accretion Characteristics," *Proc. 2018 Atmospheric and Space Environments Conference, AIAA*, (2018).

[21] Markatos, N. C., "The Mathematical Modelling of Turbulent Flows," *Appl. Math. Model.*, 10(3), pp. 190–220, (1986).

[22] Menter, F., Improved Two-Equation k-Omega Turbulence Models for Aerodynamic Flows, N*asa Sti/recon Technical Report N 93*, pp. 1–31, (1992).

[23] ANSYS Inc., *ANSYS Fluent Theory Guide*, (2018)

[24] Flack, K. A., and Schultz, M. P., "Review of Hydraulic Roughness Scales in the Fully Rough Regime," *J. Fluids Eng. Trans. ASME*, 132(4), pp. 0412031–04120310, (2010).

[25] Flack, K. A., Schultz, M. P., Barros, J. M., and Kim, Y. C., "Skin-Friction Behavior in the Transitionally-Rough Regime," *Int. J. Heat Fluid Flow*, 61, pp. 21–30, (2016).

[26] Stimpson, C. K., Asme, M., Snyder, J. C., Thole, K. A., and Mongillo, D., "Scaling Roughness Effects on Pressure Loss and Heat Transfer of Additively Manufactured Channels," *J. Turbomach.*, 139(2), p. 021003, (2017)

[27] Patir, N., "A Numerical Procedure for Random Generation of Rough Surfaces," *Wear*, 47(2), pp. 263–277, (1978).

[28] Bakolas, V., "Numerical Generation of Arbitrarily Oriented Non-Gaussian Three-Dimensional Rough Surfaces," *Wear*, 254(5–6), pp. 546–554, (2003).

[29] Spalding, D. B., "A Single Formula for the 'Law of the Wall," *J. Appl. Mech. Trans. ASME*, 28(3), pp. 455–458, (1960).

[30] Gnielinski, and V., "New Equations for Heat and Mass Transfer in the Turbulent Flow in Pipes and Channels," *Forschung im Ingenieurwesen*, 41(1), pp. 8-16, (1975).